Air shower array at the university of Puebla for the study of cosmic rays

J. Cotzomi, O. Martínez, E. Moreno, H. Salazar, and L. Villaseñor*
Facultad de Físico-Matemáticas, Benemérita Universidad Autónoma de Puebla,
Apartado Postal 1364, Puebla, Pue., 72000, México
**On leave of absence from Institute of Physics and Mathematics, University of Michoacan,*
Morelia, Mich., 58040, México

Recibido el 18 de febrero de 2004; aceptado el 15 de octubre de 2004

We describe the design and performance of an extensive air shower detector array built in the Campus of the University of Puebla (located at 19°N, 90°W, 800 g/cm^2) to measure the energy and arrival direction of primary cosmic rays with energies around 10^{15} eV, known as the knee of the cosmic ray spectrum. The array consists of 18 liquid scintillator detectors (12 in the first stage), and 3 water Cherenkov detectors (one of 10 m^2 cross section and two smaller ones of 1.86 m^2 cross section), distributed in a square grid with a detector spacing of 20 m over an area of 4000 m^2. In this paper, we discuss the calibration and stability of the array and report on preliminary measurements of the arrival directions and energies of cosmic ray showers detected with the first stage of the array consisting of 12 liquid scintillator and 3 water Cherenkov detectors. Our results show that the array is efficient in detecting primary cosmic rays with energies in the range of 10^{14} to 10^{16} eV, with an angular resolution lower than 5.5° for zenithal angles in the range of 20° to 60°. We also point out that the capability of water Cherenkov detectors to separate electromagnetic from muon components of extensive air showers. Finally we remark that this facility is also used to train students interested in the field of cosmic rays.

Keywords: Cosmic rays; arrival direction; energy spectrum.

Se describe el diseño y la operación de un arreglo de detectores de cascadas de rayos cósmicos construido en el campus de la Universidad Autónoma de Puebla (localizado a 19°N, 90°W, 800 g/cm^2) para medir la energía y dirección de llegada de rayos cósmicos primarios con energías alrededor de 10^{15} eV, conocida como "la rodilla" del espectro de rayos cósmicos. El arreglo consiste en 18 detectores de centellador líquido (12 en la primera etapa) y 3 detectores Cherenkov de agua (uno de sección transversal de 10 m^2 y dos más pequeños de 1.86 m^2 de sección transversal), distribuidos en una red cuadrada con 20 m de espacio entre los detectores sobre una área de 4000 m^2. En este artículo se discute la calibración y estabilidad de operación del arreglo y se reporta sobre las mediciones preliminares de las direcciones de llegada y de las energías de cascadas de rayos cósmicos observadas con la primera etapa del arreglo que consiste en 12 detectores de centellador líquido y 3 detectores Cherenkov de agua. Los resultados obtenidos indican que el arreglo es eficiente en la observación indirecta de rayos cósmicos primarios con energías dentro del intervalo de 10^{14} a 10^{16} eV con una resolución angular menor a 5.5° para ángulos zenitales en el rango de 20° a 60°. También se discute la capacidad de los tanques Cherenkov de agua para hacer posible una separación de las componentes electromagnética y muónica de las cascadas de rayos cósmicos. Las instalaciones de este arreglo se usan también para entrenar estudiantes interesados en el área de los rayos cósmicos.

Descriptores: Rayos cósmicos; dirección de llegada; espectro de energía.

PACS: 98.70.Sa; 29.40.Ka; 29.40.Mc

1. Introduction

The cosmic rays that can be detected at the surface of the Earth are called secondary because they are originated from the collision of primary cosmic rays against nitrogen and oxygen nuclei high in the atmosphere. These collisions give rise to extensive air showers (EAS) which penetrate the atmosphere, and can be studied with detectors on the ground. EAS are composed by: hadronic, electromagnetic, muonic and neutrino components; from which only the electromagnetic and muonic components are detected with ground detectors, because the hadronic component dies away soon after the primary collision, converting its energy into the other components, and the neutrino component does not interact. The energy spectrum of cosmic rays has been studied extensively by direct measurements with detectors on balloons and satelites for energies below 10^{14} eV, where their flux is still large enough to allow direct detection with the small detectors that can be carried above the atmosphere, and by indirect measurements with detectors on the ground for higher energies, *i.e.*, arrays of particle detectors that measure the particle flux at the Earth surface, or telescopes that measure the flux of fluorescence or Cherenkov light produced by particles in the EAS as they ionize nitrogen molecules from the atmosphere. It has been found that the cosmic ray energy spectrum is well described by a power law, *i.e.*, $dE/dx\ \alpha E^{-\gamma}$, over many decades of energy with the spectral index γ approximately equal to 2.7, and steepening to $\gamma = 3$ at $E = 3 \times 10^{15}$ eV. This structural feature, known as the "knee", has been and continues to be studied in detail with ground arrays, which measure the electromagnetic component of EAS [1].

However, the nature of the knee is still a puzzle despite the fact that it was discovered 45 years ago [2]. Most theories consider it of astrophysical origin and relate it to the breakdown of acceleration mechanisms of possible sources or to a leakage during propagation of cosmic rays in the magnetic fields within our galaxy; particularly, these theories have led to the prediction of a primary composition richer in heavy el-

ements around the knee, related to the decrease of the galactic confinement of cosmic rays with increasing particle energy. The main tool to study the composition of primary cosmic rays with ground detector arrays is by measuring the ratio of the muonic in relation to the electromagnetic component of EAS; in fact, Monte Carlo simulations show that heavier primaries give rise to a greater muon/EM ratio, compared to lighter primaries of the same energy [3]. In fact, evidence for such variations has been reported recently [4]. Alternatively, there are scenarios where a change in hadronic interaction at the knee energy gives rise to new heavy particles [5], which produce, upon decay, muons of higher energies than those produced by normal hadrons. It is therefore important to achieve a good determination of the ratio of the muonic to the electromagnetic components along with the muon energies involved for primary cosmic rays around the knee.

The extensive air shower detector array at UAP (EAS-UAP) was designed to measure the lateral distribution and arrival direction of secondary particles for EAS in the energy region of 10^{14}-10^{16} eV. In this paper, we report on preliminary results obtained by continuous operation over one year of the first stage of the array, consisting of 12 liquid scintillator detectors out of the 18 planned. Throughout this operation period, we used the water Cherenlov detectors exclusively to provide complementary data to the liquid scintillator detectors, *i.e.*, additional timing information for a better determination of the arrival direction, and additional particle flux information for a better determination of the primary energy. We also demonstrate the ability of single water Cherenkov detectors to separate single EM particles from single muons and from showers in a natural way. In a second phase of the operation of the EAS-UAP array, with the number of liquid scintillator detectors upgraded to 18, we will attempt to measure the muon/EM ratio and to estimate the energy of the muons involved by making extensive use of the information provided by the water Cherenkov detectors. The special location of the EAS-UAP array, 2200 m above sea level and all the facilities in the Campus of the Puebla University make it a valuable apparatus for the long term study of cosmic rays, and at the same time an important training center for new physics students interested in getting a first class education in the field of cosmic rays in Mexico.

2. Experimental setup

The array, located at the campus of the FCFM-UAP (19° N, 89° W, 800 g/cm^2) consists of 18 liquid scintillator detectors distributed uniformly on a square grid with spacing of 20 m, and three water Cherenkov detectors (one of 10 m^2 cross section and two smaller ones of 1.86 m^2 cross section), as shown in Fig. 1. Detectors T1-T18 are liquid scintillator detectors. The two small water Cherenkok detectors are in the same position as detectors T1 and T5. The 10 m^2 cross section water Cherenkov detector is located at 5 m from T6 in the direction toward T1. Each one of the liquid scintillator detectors consists of a cylindrical container of 1 m^2 cross

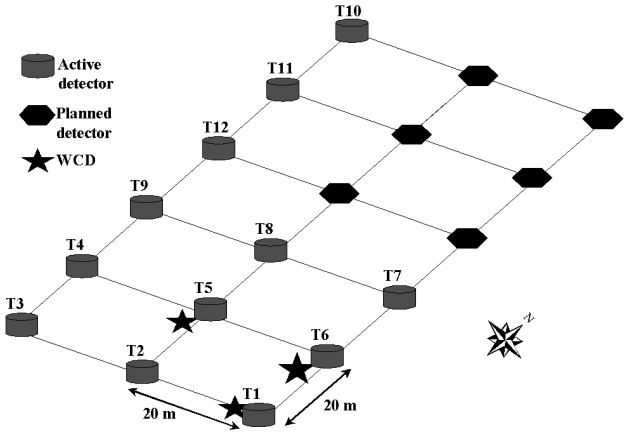

FIGURE 1. Detector layout of the Extensive Air Shower array. Detectors T1-T12 are liquid scintillation detectors. The two small water Cherenkov detectors are in the same positions as detectors T1 and T5. The 10 m^2 cross section water Cherenkov detector is located 5 m from T6 in the direction towards T1. This figure shows the position of 6 additional liquid scintillator detectors that will be added in the near future.

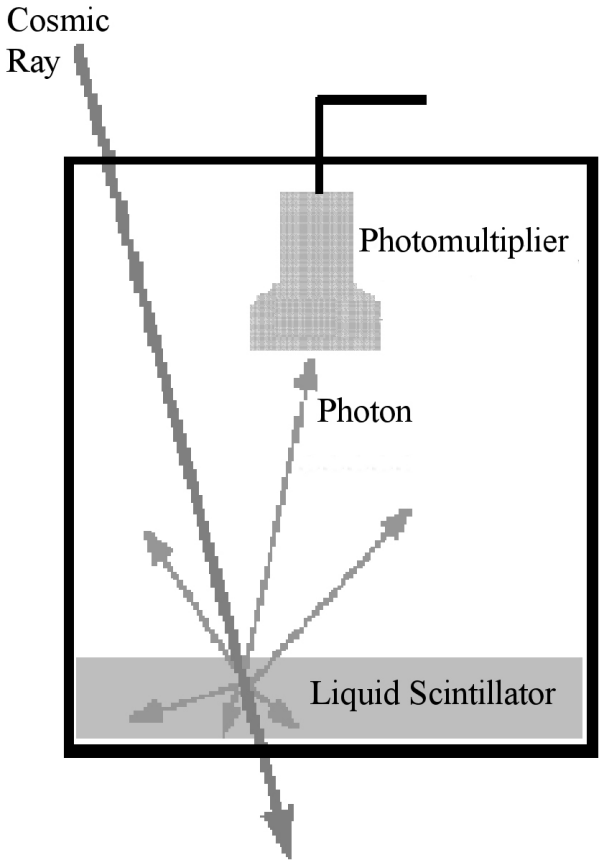

FIGURE 2. Schematic diagram of a liquid scintillator detector.

section, made out of polyethylene filled with 130 l of liquid scintillator up to a height of 13 cm; each light-tight container has a 5" photomultiplier (PMT, EMI model 9030A) located inside along the axis of the cylinder facing down, with the photo-cathode 70 cm above the surface of the liquid scintillator, as shown in Fig. 2.

We used a commercial liquid scintillator (Bicron BC-517H) consisting of a mineral oil made out of hydrogen and carbon atoms with a ratio of 1.9 hydrogen atoms per carbon atom. The large water Cherenkov detector consists of a cylindrical tank made of roto-molded polyethylene with a cross section of 10 m^2 and a height of 1.5 m. The tank, filled with purified water up to a height of 1.2 m, has three 8" PMTs (Electron Tubes model 9353K) looking downwards at the tank volume from the water surface. The three PMTs collect the Cherenkov light emitted by charged particles in the EAS as they cross the tank at speeds higher than the speed of light in water. The two small water Cherenkov detectors consist of cylindrical tanks made of polyethylene with an inner diameter of 1.54 m and a height of 1.30 m filled with 2300 l of purified water up to a height of 1.2 m. They have a single 8" PMT (Electron Tubes model 9353K) located at their center and looking downwards at the top of the water level to collect the Cherenkov light. All the inner surfaces of the three Cherenkov tanks are optically sealed and covered with a material called Tyvek, which reflects light in a highly diffusive way in the relevant wavelength range of 300-500 nm where PMTs operate more efficiently.

The array has been upgraded from 8 to 12 liquid scintillator detectors during 2003, and it has been operated in a quasi-continuous way. The trigger used requires the signals to coincide in the four central liquid scintillator detectors (T2, T4, T8 and T6), which form a rectangular sub-array with an area of 40×40 m^2. This trigger sub-array was chosen to assure that the shower core is located inside the array. The measured trigger rate is of 80 events per hour. The data acquisition system consists of a set of 9 two-channel digital oscilloscopes (Tektronix model TDS 220) that digitize the signals from the 12 PMTs of the 12 liquid scintillator detectors and the 5 PMTs from the 3 water Cherenkov detectors. All the digital oscilloscopes are connected to the GPIB port of a PC in a daisy chain configuration. The system is controlled by a PC running a custom-made acquisition program written in a graphical language called LabView [6]. We used commercial NIM modules to discriminate the PMT signals at a threshold of -30 mV (LeCroy NIM discriminator modules Octal 623B and Quad 821), and to generate the coincidence trigger signal (LeCroy NIM coincidence unit model 465).

3. Results and discussion

Monitoring and calibration of all the detectors is essential for the correct operation of the detector array which was designed to be operated remotely with minimal maintenance. Therefore, simple, reliable and cost-efficient monitoring and calibration methods are required.

3.1. Monitoring

A method based on single-particle rates was used as a simple estimator of the operation stability in the first detector arrays built around the world. Modern technology, however, allows the use of more detailed information on the detector response to single particles and EAS. In our case, we use a CAMAC scaler (CAEN 16 ch scaler model C257) to acquire the individual single-particle rates of each detector into the PC through the GPIB port (LeCroy model 8901A CAMAC-GPIB controller on the CAMAC crate and a National Instruments GPIB card on the PC), as shown in Fig. 3, for 9 liquid scintillator detectors. These rates were used to monitor the stability and performance of the array. The single-particle rates of our detectors do show a slight day-night variation smaller than 10% due to temperature variations in the electronics. The rate distributions also show, see Fig.3, dispersions around the central value of about 3% (the maximum was rms/mean=2.8% for detector T2). Likewise, our DAQ system acquires all the PMT traces for each triggered event. An example of the front panel of this DAQ program is shown in Fig. 4 for 10 of the 12 liquid scintillator detectors. The acquired traces are used by the PC to perform on-line measurements of the integrated charges, arrival times, amplitudes and widths of all signals from the 17 PMTs, these data are saved into a hard-disk file for further off-line analysis. As can be seen from Fig. 4, the typical width of extensive air shower signals detected by each scintillator detector is around 25 ns.

3.2. Calibration

Calibration of the detectors is essential as it enables us to convert the information from the electronic signals measured in each detector into the number of particles in the EAS that reach the detectors, and finally into the energy of the primary cosmic ray. As traditionally done, we use the natural flux of background muons and electrons to calibrate our detectors. For the location of the EAS-UAP, muons are the dominant contribution to the flux of secondary cosmic rays for energies above 100 MeV with about 300 muons per second per m^2, and a mean energy of 2 GeV; at lower energies, up to 100 MeV, electrons dominate with a flux 1000 times greater and a mean energy around 10 MeV [7]. These secondary particles originate in the atmosphere from hadronic interactions of low energy primary cosmic rays, and provide a reference constant in time suitable to unfold other variations in our apparatus. In particular, we record, on a continuous basis, the energy depositions of single particles crossing the detectors in arbitrary directions by means of a special trigger called "calibration trigger", which requires single signals above threshold on individual detectors and operates simultaneously with the coincidence trigger so that we obtain the right calibration constants for each detector, *i.e.*, the constants derived from the calibration events in the 10 minute period before the occurrence of each shower event. We use these calibration runs to obtain the spectra of energy depositions of single particles, as shown in Fig. 5 for 6 out of the 12 liquid scintillator detectors, and in Fig. 6 for one of the small water Cherenkov detectors. Liquid scintillator detectors are more sensitive to low energy particles (dE/dx is proportional to the inverse of

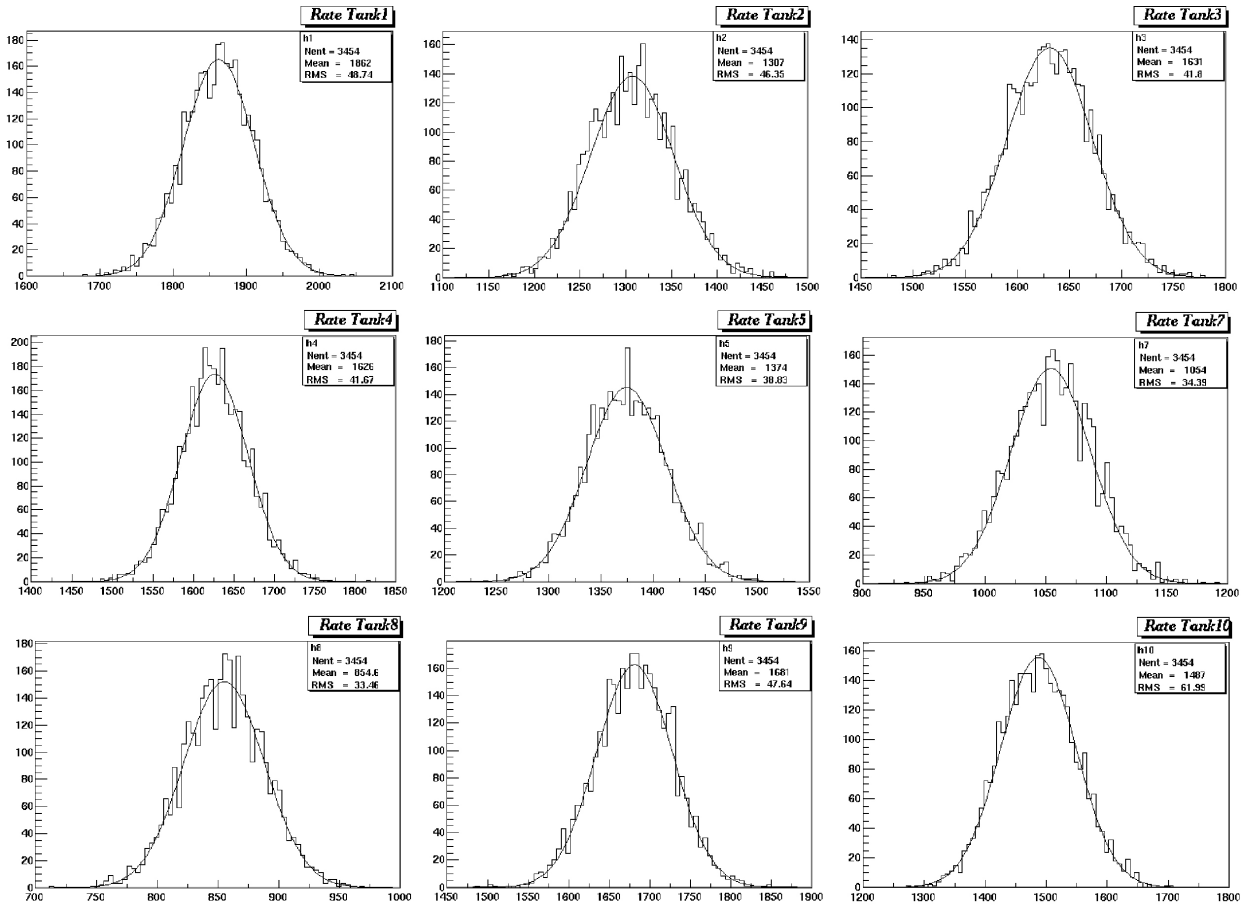

FIGURE 3. Single particle rate distributions of 9 liquid scintillator detectors obtained by the CAMAC-based monitoring system. The horizontal axis is in units of 0.1 Hz, and the typical values for rms/mean are lower than 3%.

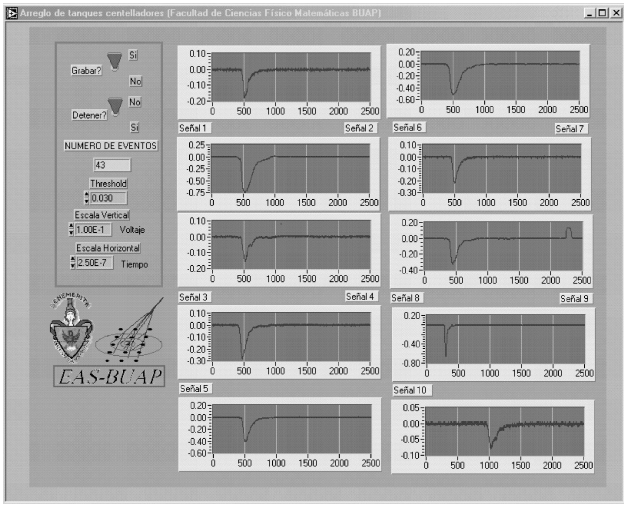

FIGURE 4. Oscilloscope traces of 10 PMT signals of 10 liquid scintillator detectors for a trigger event as displayed by the DAQ program. The vertical scale is in V_0H and the horizontal units are 0.1 ns, *i.e.* typical signals are around 25 ns wide. The lack of synchronization of the PMT signals is due to the varying cable lengths of the detector PMTs, and this effect on the determination of the arrival direction of the air showers is corrected off-line.

the squared velocity of charged particles reaching scintillator detectors), while Cherenkov detectors are more sensitive to relativistic muons and electrons. It is important to keep in mind that a 2 GeV muon can cross the detector (dE/dx is around 2 MeV/cm) whereas a 10 MeV electron cannot; therefore muons produce more Cherenkov light than lower energy electrons (the range of 10 MeV electrons in a water-like liquid is about 5 cm).

In the case of the water Cherenkov detectors the signals of muons crossing the detectors are proportional to their geometric path lengths. The second peak in Fig. 6 corresponds to the mean PMT charge deposited by muons crossing the detector in arbitrary directions, while the first peak corresponds to corner-clipping muons and also EM particles that produce smaller signals. For water Cherenkov detectors, the conversion of the mean charge of the second peak into a useful parameter is carried out by means of a control experiment, as shown in Fig. 7 for one of the two small water Cherenkov detectors. The two scintillation hodoscopes above and below the detector let us to determine the position of the charge peak for muons crossing the detector vertically. We call this paramenter a vertical equivalent muon (VEM). Our measurements indicate that 1 VEM is equal to approximately 0.92 times the position of the second peak in the charge distribution, in Fig. 6 [8]. In the case of the liquid scintillator detectors the second peak is dominated by electrons that fully deposit their energy, and its position also corresponds closely

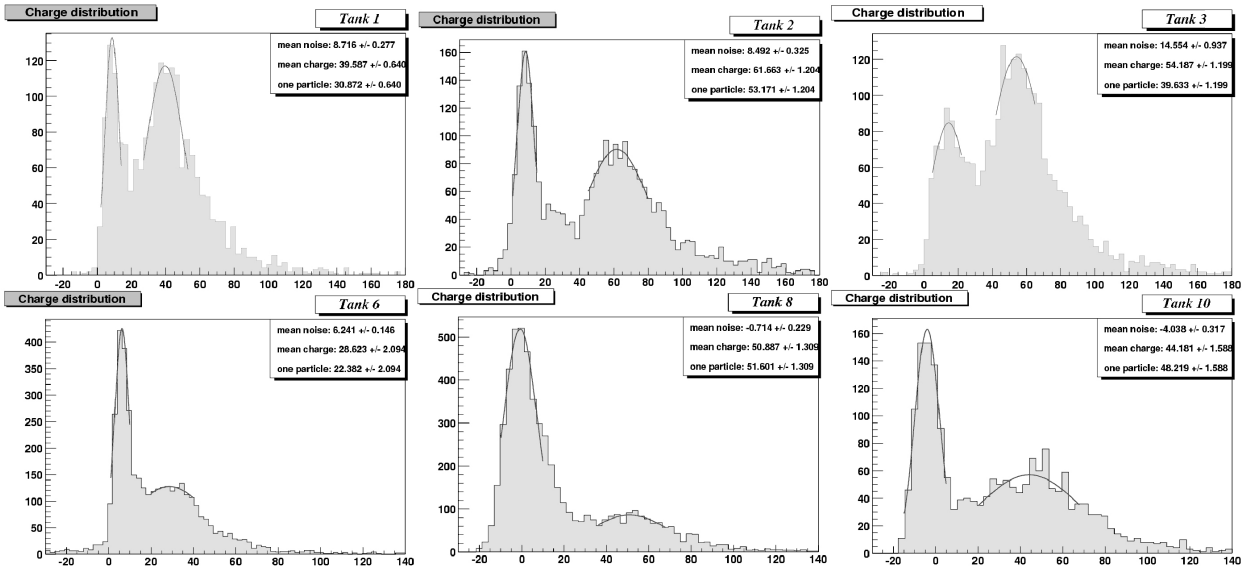

FIGURE 5. Charge distribution of single particles as measured by 6 of the 12 liquid scintillator detectors, the vertical scale is in arbitrary units and the horizontal in pC. The first peak corresponds to noise and the second to the signal of single particles, i.e. muons and electrons. The mean charge of single particles is given by the difference of the mean values of the two Gaussian fits.

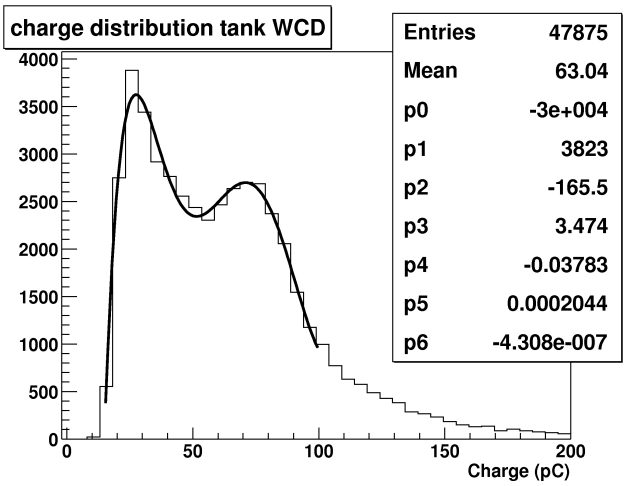

FIGURE 6. Charge distribution of single particles as measured by one of the two small water Cherenkov detectors. The vertical scale is in arbitrary units and the horizontal in pC . The position of the second peak gives the mean charge deposited by muons crossing the detector vertically. The first peak is an artifact of the threshold used by the discriminator. The insert shows the values of the parameters of the polynomial fit.

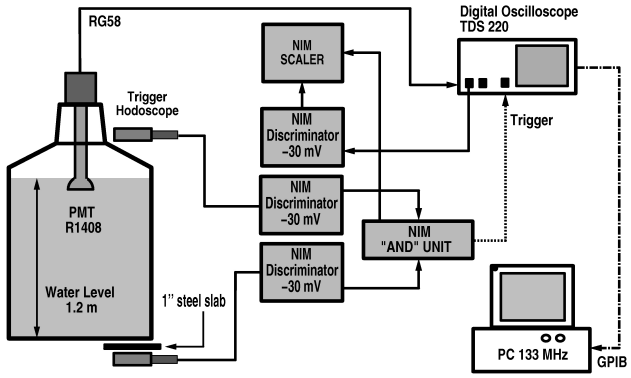

FIGURE 7. Experimental setup used to obtain the charge deposited by vertical muons and to obtain the value of one VEM in terms of the position of the second peak shown in Fig. 6.

to one equivalent particle. In consequence, we have a reliable way of converting the charge deposited in each detector into a number of equivalent particles (electrons for liquid scintillator and muons for water Cherenkov detectors) [9].

3.3. Arrival direction

The direction of the primary cosmic ray is inferred directly from the relative arrival times of the shower front at the different detectors. Figure 8 illustrates the way in which the arrival times at each detector depend on the arrival direction of the shower front. Figure 9a shows the measured zenithal distribution obtained from data of the first year of operation. The solid line corresponds to the function $dI/d\Omega = A\cos^{6.6}\theta\sin\theta$ obtained as the best fit to the data, the fitted curve agrees with the literature [10]. Figure 9b shows the measured azimuthal distribution which is in agreement with a flat distribution (solid line), *i.e.*, the showers we detect do not present any east-west modulation due to the effect of the magnetic field of the Earth as cosmic rays of lower energies do. We also verified that no artifact biases on the angular distribution is introduced by our trigger scheme by checking that the distributions for the time differences between the arrival time and the trigger coincidence time are centered around cero for each of the four detectors used in the trigger system.

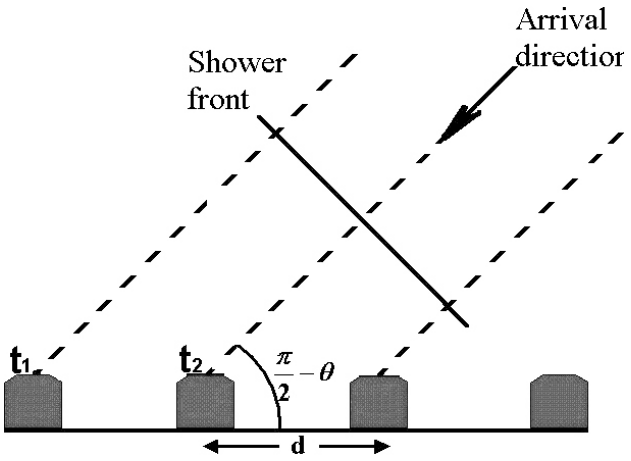

FIGURE 8. Illustration of the dependance of the arrival times of the particles in the shower front with the arrival direction. In the approximation of a flat shower front the formula $\sin\theta\sin\phi = c(t_2 - t_1)/d$ relates the arrival times, t_1 and t_2, of the shower front detected in two adjacent detectors separated by a distance d with the zenithal and azimuthal angles, θ and ϕ, respectively, of the direction perpendicular to the shower plane traveling at the speed of light c.

In order to estimate the angular resolution of the EAS-UAP detector array, we assume, as a good approximation, that the front of the EAS is a flat disk perpendicular to the direction of the primary cosmic ray. Therefore, if the arrival times of the shower front detected in two adjacent detectors separated by a distance d are t_1 and t_2, then, the normal direction to the shower front is, in this approximation, given by the formula:

$$\sin\theta\sin\phi = \frac{c(t_2 - t_1)}{d}$$

where θ and ϕ are the zenithal and azimuthal angles of the vector normal to the shower plane traveling at the speed of light c. Assuming that the errors in θ and ϕ are equal, we can therefore write the error in θ as,

$$\Delta\theta = \sqrt{2}\left[2\left(\frac{c}{d\Delta t}\right)^2 + \frac{1}{2}\left(\frac{\Delta d}{d}\right)^2 \sin^2\theta\right]^{1/2}$$

where we have averaged out the azimuthal angle by using $\langle\cos^2\phi\rangle = \langle\sin^2\phi\rangle = 1/2$; Δt and Δd are the errors in the arrival time and the distance determination of the shower particles; $\Delta t = (\sigma_i^2 + \sigma_{sh}^2)^{1/2}$, where σ_i is our intrinsic resolution in the time measurement and σ_{sh} is the root mean square in the arrival time of shower particles due to the finite thickness of the EAS disk. In order to estimate σ_{sh}, we use the formula proposed by Linsley [11] which parametrizes the shower thickness as a function of the distance of the detector from the shower core, r, as:

$$\sigma_{sh} = (1.6\text{ ns})(1 + r/30)^{1.65}/\sqrt{\{n(r,\theta)\}}$$

where r is in meters, and $n(r,\theta)$ is the number of particles crossing the detector located at a distance r from the core

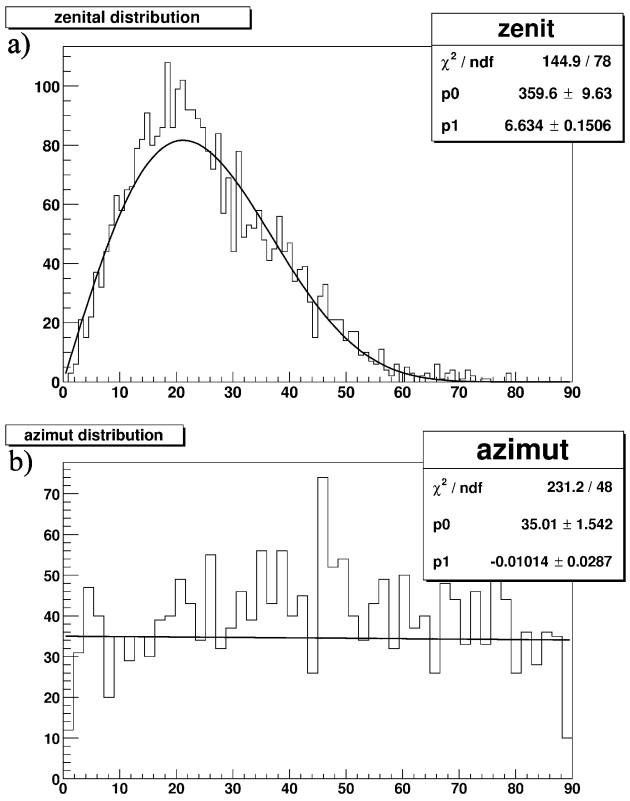

FIGURE 9. a) Zenithal angle distributions of EAS measured with the EAS-UAP detector array. The units of the horizontal axis are degrees. The solid line corresponds to the function $dI/d\Omega = A\cos^{6.6}\theta\sin\theta$ obtained as the best fit to the data, the fitted curve is in good agreement with the literature. The insert gives the fitted values; p0 is equal to A, and p1 is the exponent of $\cos\theta$. b) Measured azimuthal distribution. The units of the horizontal axis are degrees. The fitted curve is $P_0 + P_1\phi$ where P_0 and P_1 are given in the insert. We checked that the distribution is in agreement with a flat distribution (solid line) over the whole 2π range of the azimuthal angle ϕ.

of the shower with zenith angle θ. In our case, with 1 m^2 surface detectors, $n(r,\theta)$ is the shower particle density given by the NKG formula:

$$\rho(S,r) = K(S)(r/R_0)^{S-2}(1 + r/R_0)^{S-4.5}[12],$$

where S is the shower age, r the distance of the detector to the shower core, and R_0 is the Molliere radius (90 m for an altitude of 2200 m a.s.l.). If we neglect the slight dependence on θ in the expression for σ_{sh}, we can rewrite the expression for $\Delta\theta$ as,

$$\Delta\theta = \sqrt{2}\Big\{2(c/d)^2\left[\sigma_i^2 + 2.56(1 + r/30)^{33}/n(r)\right] + \frac{1}{2}(\Delta/d)^2\sin^2\theta\Big\}^{1/2}$$

From this expression, we can see that the error due to the shower thickness dominates for large values of r, while near

the shower core the intrinsic time resolution of the timing measurement is the dominant contribution, which in our case is 2.7 ns. Specifically, for 1m^2 detectors separated by 20 m, and a zenith angle of 20°, a typical shower may have a particle density of 50/m^2 at the core, and thus we obtain $\Delta\theta = 5.1°$. Likewise, for $\theta = 60°$ we obtain a resolution $\Delta\theta$ of 5.5°.

3.4. Energy determination

We determine the number of particles in each detector using the single-particle charge spectrum discussed in Sec. 3.2. The core position, lateral distribution function, and total number of shower particles N_e are reconstructed from a fit of the NKG expression given above for the electron lateral function to the particle densities recorded by the different detectors on an event-by-event basis. Finally, the shower energy is obtained by using the relation $N_e(E_0) = 117.8\ E_0^{1.1}$, where E_0 is the energy of the primary cosmic ray expressed in TeV (13,14). Figure 10 shows the measured particle densities and the fitted lateral distribution for two examples of vertical showers. The reconstructed energies for the events of Fig. 10a and 10b were 2.3×10^{16} eV and 3.6×10^{16} eV, respectively. Figure 11 shows the differential distribution, dN/dN_e, of the shower size, N_e, obtained for vertical showers. The fitted slope found is 2.44 ± 0.13, which corresponds to a spectral index $\gamma = 2.6$ in the energy spectrum $dN/dE\alpha E^{-\gamma}$, *i.e.*, in agreement with the literature (13).

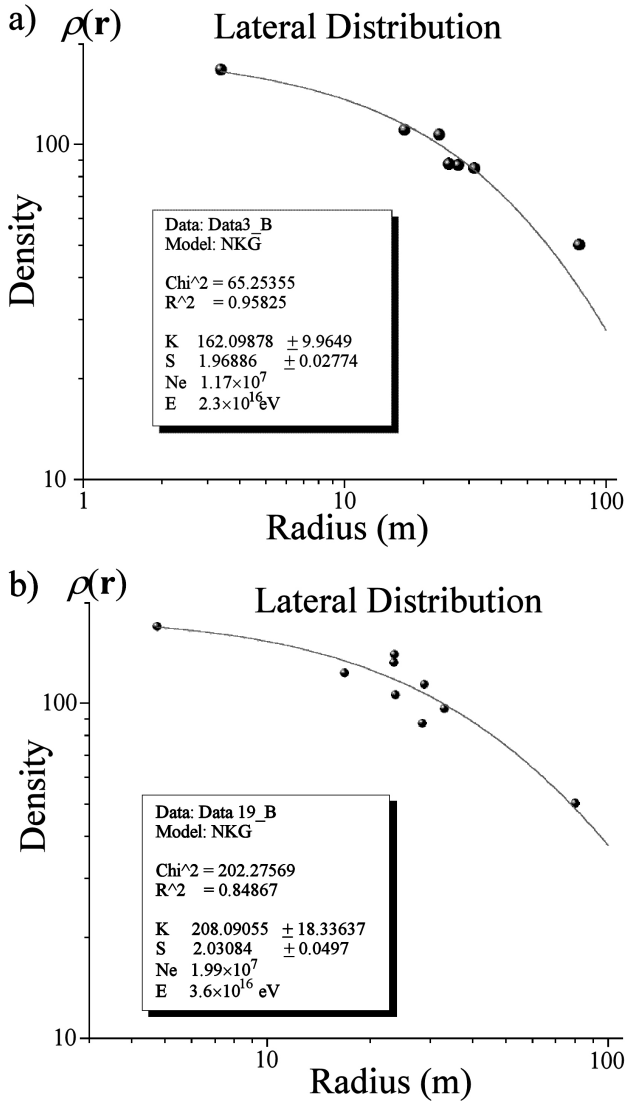

FIGURE 10. Lateral distribution function fitted to the measured particle densities for two examples of extensive air showers. The reconstructed energies for these events were 2.3×10^{16} eV and 3.6×10^{16} eV for Fig. 9a and Fig. 9b, respectively. The insert shows the values of the parameters of the fitted NKG curve: K is a scale factor, s is the age of the shower, N_e and E are the number of particles and the energy, respectively.

3.5. Muon/EM separation

Finally, we would like to discuss work in progress which points to the possibility of using some structural features of the oscilloscope traces of water Cherenkov detectors to separate the different components of EAS, with the aim of determining the mass composition of the primary cosmic ray. We have obtained inclusive signals produced by secondary cosmic rays by using an inclusive trigger which requires a simple amplitude threshold of -30 mV in any of the two small water Cherenkov detectors. This trigger selects events that occur locally at each water Cherenkov detector (*i.e.*, isolated particles or local showers of low energy $\sim 10^{11}$ eV) with charge values above 0.08 VEMs. The oscilloscope traces of single-

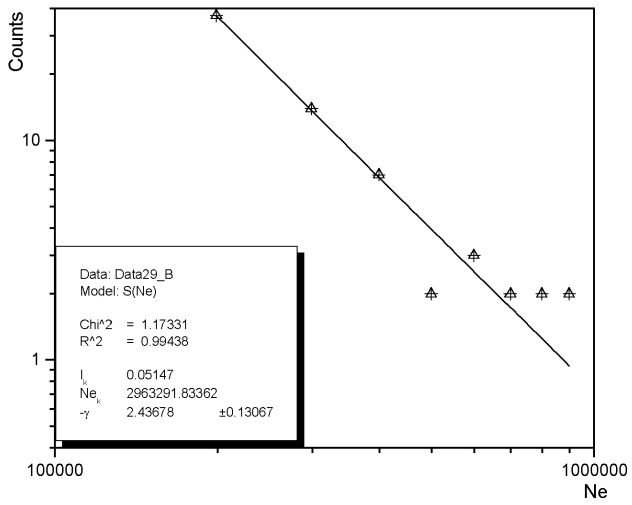

FIGURE 11. Distribution of the shower size, N_e, obtained for vertical showers. The fitted curve is $I_k(N_e/N_{ek})^{-\gamma}$, where N_{ek} is the number of particles at the knee and I_k the flux at the knee, the insert shows their fitted values, in particular the fitted value for $\gamma = 2.44 \pm 0.13$ corresponds to a spectral index $\gamma = 2.6$ as explained in the text, in good agreement with the value reported in the literature for the energy spectrum $dN/dE\alpha E^{-}\gamma$.

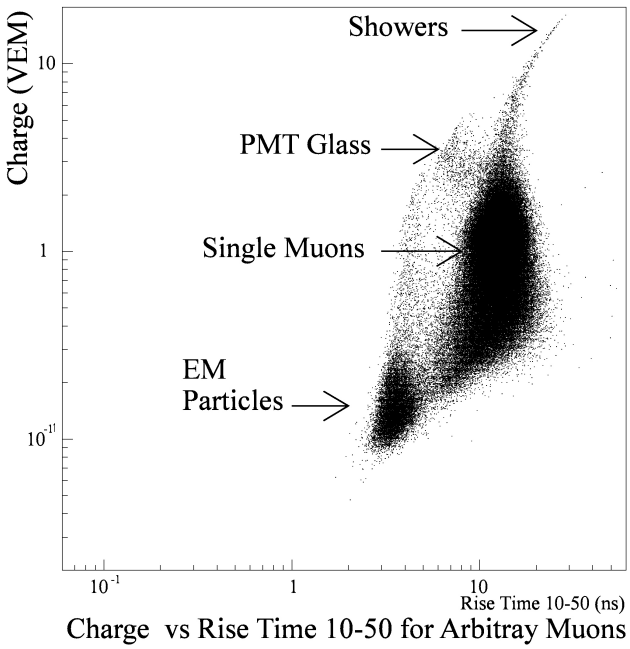

FIGURE 12. Charge in VEM vs rise time from 10% to 50% in ns for inclusive cosmic ray signals in one of the two small water Cherenkov detectors. The separation into EM particles, single muons, showers and the interaction of muons with the PMT glass is evident in these plots.

detector events are used to perform off-line measurements of the charge, rise time 10%-50%, rise time 10%-90%, and amplitude for each event. Figure 12 shows a plot of the amplitude versus the rise time from 10% to 50% for these events. This plot shows that the events separate naturally into the following groups of signals associated to secondary cosmic rays: isolated EM particles, isolated muons, interaction of isolated muons with the glass envelope of the PMT, and extensive air showers. We have also found other bi-dimensional parametric spaces that produce equally good separation, such as charge vs amplitude, amplitude vs rise time, and amplitude vs charge/amplitude. Identification of the traces of isolated electrons and muons enable us to form artificial traces for EAS with known values of muon/EM. These artificial signatures for EAS can, in turn, be used on a number of classification schemes, for instance neural networks, to measure the muon/EM value of true showers. This work is reported in detail in Ref. 15. In the near future, we will analyze the signals of the water Cherenkov detectors with liquid scintillator signals for EAS to attempt to estimate the muon contents of EAS on a one to one basis.

4. Conclusion

We have described the design and operation of the first stage of the EAS-UAP detector array located in the campus of the University of Puebla. Analysis of the EAS-UAP data collected so far allows us to conclude that the detector array shows good stability with a typical dispersion of rms/mean for the rate of liquid scintillator detectors lower than 3%. The data acquisition system that we implemented, using commercial NIM and CAMAC electronics, can operate during extensive periods of data taking. The typical width of extensive air shower signals detected by our scintillator detectors is around 200 ns. We have implemented a reliable way of calibrating the detectors to perform the conversion of the charge deposited in each detector into a number of equivalent particles. We have measured the zenithal angular distribution, and found that it can be fitted by the function $\mathrm{A}\cos^{6.6}\theta\sin\theta$, in agreement with the literature. We have estimated the angular resolution in our determination of the zenithal angle to be lower than 5.5° in the range from $20^\circ < \theta < 60^\circ$. The differential distribution, dN/dN_e, of the shower size, N_e, obtained for vertical showers corresponds to a spectral index $\gamma = 2.6$ in the energy spectrum $dN/dE\alpha E^{-\gamma}$, *i.e.*, also in agreement with the literature.

Finally, we have shown that water Cherenkov detectors possess the potential to separate different signals associated to secondary cosmic rays, such as isolated EM particles, isolated muons, and extensive air showers, this is done by using structural features of the signals from these detectors and by plotting amplitude versus rise time from 10% to 50%, or other pairs of parameters such as charge vs amplitude, amplitude vs rise time and amplitude vs charge/amplitude. In the near future we will increase the number of liquid scintillator detectors to 18 to improve our aperture. During the next period of operation, we will measure the muon/EM ratio and will estimate the energy of the muons involved by making more extensive use of the information provided by the water Cherenkov detectors. The special location and the *in-situ* facilites associated to the UAP campus make the EAS-UAP array a valuable apparatus for the long term study of cosmic rays in Mexico. Besides, we also use this detector facility to educate and train new physics students interested in the field of cosmic rays.

Acknowledgments

The authors are grateful to FERMILAB for providing the liquid scintillor and to the ICFA Instrumentation Center in Morelia for providing some of the electronics required by this project. This work was partially supported by BUAP, CIC-UMSNH and CONACyT under projects G32739-E and G38706-E.

1. S.P. Swordy *et al.*, *Astroparticle Physics* **18** (2002) 129.
2. G.V. Kulikov and G.V. Khristiansen, *Sov. Phys. JETP* **41** (1959) 8.
3. B. Alessandro *et al.*, *Proc.27th ICRC* **1** (2001) 124.
4. KASCADE Collaboration (Klages H. O. *et al.*), *Nucl. Phys. B* (Proc. Suppl.), **52** (1997) 92.
5. A.A. Petrukhin, *Proc. XIth Rencontres de Blois "Frontiers of Matter"* (The Gioi Publ., Vietnam, 2001) 401.
6. National Instruments Catalog (2004).
7. J.F. Ziegler, *Nucl. Instrum and Meths.* **191** (1981) 419.
8. M. Alarcón *et al.*, *Nucl. Instrum and Meths. in Phys. Res. A* **420** (1999) 39.
9. M. Aglietta *et al.*, *Nucl. Instr. and Meth. A* **277** (1989) 23.
10. A.A. Ivanov *et al.*, *JETP Lett* **69** (1999) 288.
11. J. Linsley, *J. Phys. G* **12** (1986) 51.
12. J. Nishimura, *Handbuch der Physik XLVI/2* (1967) 1.
13. EAS-TOP Collaboration and MACRO Collaboration, *Phys Lett B* **337** (1994) 376.
14. J. Knapp and D. Heck, *Report FZKA KfK* **5196B** (1993) 8.
15. L. Villaseñor, Y. Jerónimo, and H. Salazar, *Use of Neural Networks to Measure the Muon Contents of EAS Signals in a Water Cherenkov Detector*, (Proc. of the 28th International Cosmic Ray Conference), T. Kajita, Y. Asaoka, A. Kawachi, Y. Matsubara and M. Sasaki (eds.), **1**, HE Sessions, Universal Academy Press, Inc., Tokyo, Japan, (2003) 93-96.